BCSIR

Available online at www.banglajol.info/index.php/BJSIR

Bangladesh J. Sci. Ind. Res. **60(3)**, 169-182, 2025

BANGLADESH JOURNAL OF SCIENTIFIC AND INDUSTRIAL RESEARCH

ISSN. 0304-9809

Temporal trends in shoreline dynamics with forecasting and coastal vulnerability assessment of kuakata area, Bangladesh

M. Z. R. Chowdhury and M. Helal*

Institute of Marine Sciences, University of Chittagong, Chittagong-4331

ARTICLE INFO

Received: 15 May 2025

Revised: 30 July 2025

Accepted: 14 July 2025

eISSN 2224-7157/

DOI: https://doi.org/10.3329/bjsir.v60i3.81694

ABSTRACT

This study examines the spatiotemporal dynamics of shoreline changes along the Kuakata coast, Bangladesh, over a 30-year period (1991–2021), using geospatial techniques and remote sensing data. Multi-temporal Landsat imagery, including Landsat7ETM, Landsat7ETM+, Landsat8, and 9(OLI), and the Digital Shoreline Analysis System (DSAS) were employed to quantify rates of erosion, accretion, and overall shoreline movement. The highest erosion rate was observed in the central BC part (-13.8 m/year), while the southeastern zone exhibited the highest accretion rate (+25.58 m/year). The total land loss and gain during the study period were calculated at 8 km² and 4.7 km², respectively. Temporal analysis revealed average shoreline movements of -9.68 m/year (1991–2000), -0.98 m/year (2000–2010), and +2.1 m/year (2010–2021). Erosional rates for these periods averaged -13.11 m/year, -6.42 m/year, and -8.38 m/year, while accretion rates were 15.09 m/year, 14.73 m/year, and 18.56 m/year, respectively. Our findings provide actionable insights into erosion mitigation and sustainable coastal management strategies for one of Bangladesh's most dynamic and vulnerable shorelines.

Keywords: Shoreline; Erosion; Accretion; Forecasting; Sustainable management; Remote sensing technique

Introduction

Shorelines are dynamic, constantly shifting due to factors like winds, waves, tides, sediment availability, sea level changes, and human activities (O'Brien *et al.* 2014). These changes often alternate between erosion and accretion, with land moving inward or outward over time (Alam *et al.* 2014). In the Meghna Estuary, hydrodynamic factors such as river discharges, sediment loads, tidal forces, and cyclonic surges drive ongoing landform change (Alam *et al.* 2014). Bangladesh's coastal zone, spanning 29,000 square kilometers, is highly vulnerable to rising sea levels, saltwater intrusion, erosion, and cyclonic flooding (Goswami *et al.* 2022). Rapid landform changes in this region are driven by sea level rise and wave action (Hoque *et al.* 2021), threatening tourist spots and critical infrastructure like the country's only lighthouse (Anwar *et al.* 2022). Despite these challenges, earlier research has not fully explored the impacts of sea level rise on the eastern coast of Bangladesh (Anwar *et al.* 2022).

Shoreline changes in Bangladesh result from a combination of natural and anthropogenic factors, including sea level rise, wave activity, monsoon patterns, cyclones, and human interventions like embankment construction and resource extraction (Uddin *et al.* 2020; Brammer, 2014). The Ganges-Brahmaputra Delta, home to over 129 million people, faces significant risks from sea level rise, with projections suggesting a loss of 20% of Bangladesh's land by 2100, displacing 15 million people (Paul and Rashid, 2016; Sarwar and Woodroffe, 2013). The population of

*Corresponding author's e-mail: 19901005@std.cu.ac.bd

Bangladesh has increased from 144 million in 2011 to 165.16 million in 2022, according to the latest population and housing census, and is projected to reach 175 million by 2024 (BBS, 2022; MacroTrends, 2024) with many living in low-lying floodplains vulnerable to monsoon flooding and tidal surges (BBS, 2011). The global average sea level rose by 0.21 meters from 1902 to 2015, but the Ganges Delta has experienced a much higher rate of 5–15 mm per year (Mullick *et al.* 2019; Anwar *et al.* 2022).

Tidal dynamics play a critical role in shoreline changes, particularly in Bangladesh's semi-diurnal tidal regime, where two high and two low tides occur daily (Rose and Bhaskaran, 2017). They, additionally, mentioned that the average tidal range is 1.86 to 2.47 meters, transitioning from microtidal to mesotidal conditions. Tide data, sourced from UHSLC Stations (2024) and the Bangladesh Tide Table, is essential for accurate shoreline delineation, especially when considering neap and spring tides. Spring tides, representing the highest flood levels, and neap tides, the lowest, help avoid biases in shoreline change analysis (UHSLC, 2024).

Remote sensing and GIS technologies, such as Landsat imagery and the Digital Shoreline Analysis System (DSAS), are essential for monitoring shoreline changes (Himmelstoss *et al.* 2021; Bushra *et al.* 2021). DSAS Tool, widely accepted for statistical analyses, includes a number of methods, including WLR (Weighted Linear Regression), LRR (Linear Regression Rate), NSM (Net Shoreline Movement), etc. Tools like Sentinel-2 imagery and water indices (e.g., NDWI, MNDWI) enable accurate shoreline extraction and analysis (Astiti *et al.* 2019; Fejjari *et al.* 2023). Studies have used these methods to analyze shoreline changes over decades, employing statistical techniques like linear regression to predict future trends (Crowell *et al.* 1997; Maiti and Bhattacharya, 2009).

This study focuses on Kuakata Beach, a vulnerable area in south-central Bangladesh, to analyze shoreline changes over the past 30 years using Landsat imagery, GIS, and DSAS. The Landsat images for analysis are collected from USGS Earth Explorer (https://earthexplorer.usgs.gov). This research highlights the critical need for integrated geospatial analyses and field validation in understanding coastal dynamics. By integrating tide data and advanced remote sensing techniques, the study aims to provide insights into erosion, accretion, and shoreline stabilization processes, contributing to effective coastal management and policy development.

This research attempts to assess quantitative factors, including annual shoreline movement rate, land loss and land gain over 30 years from 1991 to 2021, and find vulnerable and critical areas by predicted graphical shoreline visualization, by integrating GIS and Remote Sensing techniques.

Materials and methods

Study area

The dynamic coastal region of Bangladesh, situated at the southernmost area along the Bay of Bengal, is continuously deformed by multiple factors, including sediment accumulation from three mighty rivers source; Ganges River, the Meghna River, and the Brahmaputra, wave action, etc. The deltaic stability majorly depends on the sediment deposition and becomes a shelter for biodiversity. Kuakata sea coastline is situated in the central zone of the coast of Bangladesh, which contains two major estuaries: the estuaries of Andarmanik River at the western zone, and the estuaries of Golachipa River at the eastern portion (Fig. 1). This study area belongs to Kalapara Upazila in the Patuakhali district, and it covers from 21° 48' 33.23" N to 21° 52' 16.03" N latitude and 90° 6' 16.45" E to 90° 12' 48.46" E longitudes (Fig. 1). The study area get experience the high- est temperature in January (25.1°C) and 33.8°C in April (BMD, 2020), with a mean annual rainfall of 2580 mm/year.

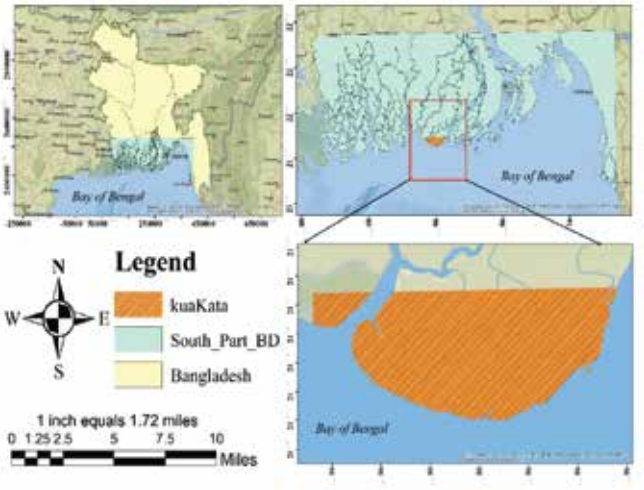

Fig. 1. Location map of the central southernmost area of Bangladesh

The variation of wave height can be observed based on two major season, during monsoon season, the wave height is typically around 1.8m, on the other hand, during the summer season from January to March, the wave height is very small; however, in general, the wave height stays 1m. Tides in the beach region are semi-diurnal, with daily tide levels ranging from 1 to 1.5 m (Uddin and Niloy, 2022).

Data source

Multi-temporal Landsat images, including TM, ETM+, and OLI/TRIS sensors, were utilized from 1990 to 2021 to analyze the shoreline dynamics of Kuakata. Specifically, four satellite images were selected at 10- Multi-temporal Landsat images, including TM, ETM+, and OLI/TRIS sensors, were utilized from 1990 to 2021 to analyze the shoreline dynamics of Kuakata. Specifically, four satellite images were selected year intervals from 1991 to 2021 (as shown in Table I). The images were acquired from reliable platforms such as USGS Earth Explorer (https://earthexplorer.usgs.gov) and GLOVIS (www.glovis.gov.us), ensuring a cloud cover of less than 5% to maintain data quality and accuracy (Islam *et al.* 2022).

$$Uncertainty(U) = \sqrt{\frac{E_{current} + E_{next}}{Year\ Gap}} \quad (1)$$

Here, $E_{Current}$ represents the total positional error for the current year, and E_{Next} represents the total positional error for the following year.

All the metadata of satellite images are shown in Table I. To ensure accuracy in shoreline change detection, tide data were collected from two main sources: UHSLC (2024) and Bangladesh Tide Times (2024). The uncertainty in shoreline position for each time interval was calculated using Equation 1 (Himmelstoss *et al.* 2021), and the values are added in Table 1.

Data preparation

Four key steps were used to study the changes along the shoreline. These steps included: (1) processing images with Arc-GIS, which involved correcting the images and calculating the NDWI to separate the images into water and non-water categories, (2) using Otsu's Binary Thresholding to create a binary image and to outline the shoreline between water and non-water areas, (3) estimating the errors in the LANDSAT images, and (4) using DSAS to measure the statistics of the changes (Mullick *et al.* 2019). Shoreline change is measured using the WLR, EPR, and LRR methods. This study looked at the dividing line between land and water by using a binary threshold method. While separating the land pixels from the water pixels, the shoreline was identified without including the tidal wave. As a result, the land boundary line considered in this study is less likely to have been mistakenly caused by waves and tides. To calculate the rate of shoreline change, we looked at four different shorelines from the study area over 30 years: 1991, 2000, 2010, and 2021. Where inconsistency has been found, the shoreline has been digitized on a scale of 1:1000, which indicates a very high accuracy (Kabir and Tanvir, 2020). Table II displays major attributes regarding shorelines and baselines, including their length, uncertainty, date, etc.

The baseline has been taken 200 meters away from the most ancient shoreline position, and transect spacing has been chosen to be 150m, where the number of transects is 179 along the coastline.

Image correction

Landsat imagery captures pixel values as digital numbers (DN), which, as highlighted by (Chander *et al.* 2009) Top-Of-Atmosphere (TOA, serve as the foundation for radiometric adjustments that convert raw satellite data into calibrated units like radiance or reflectance, ensuring consistency and precision for scientific analyses across varying sensors, times, and atmospheric conditions.

Table I. Showing major metadata for four different satellite images

Satellite	Seasonal Error	Spatial resolution	Pixel Error	Tide Gauge(m)	Digitation Error	Uncertainty
Landsat 8	0	30	0	0.95	15	7.02
Landsat 7	0	30	0	0.62	15	6.33
Landsat 7	0	30	0	1.80	15	5.77
Landsat 8	0	30	0	1.50	15	2.11

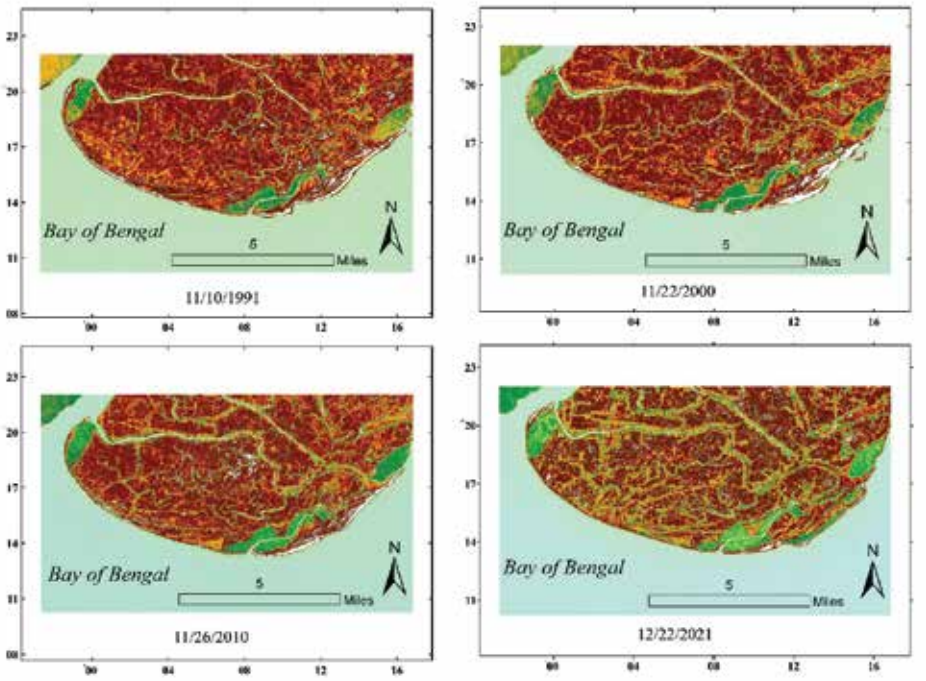

Fig. 2. AOI (Area of Interest), cutting from four selected Satellite images

Chander *et al.* (2009) Top-Of-Atmosphere (TOA suggested changing DN to Radiance for images taken by the Landsat MSS, TM, and ETM sensors by using these equations (2, 3).

$$L_\lambda = \frac{LMAX_\lambda - LMIN_\lambda}{Q_{calmax} - Q_{calmin}}(Q_{cal} - Q_{calmin}) + LMIN_\lambda \quad (2)$$

Where Lλ is the radiance of a spectral unit of"W/(m2 sr. μ m)," Qcal is the pixel value of quantized calibrated [DN], Q_{calmin} is the Minimum Q_{cal}, Q_{calmax} is the Maximum Q_{cal}, $LMIN_\lambda$ = Minimum L_λ scaled to Q_{calmin} [W/(m2 sr μm)], $L_{MAX\lambda}$ = Maximum L_λ scaled to Q_{calmax} [W/(m^2 sr μm)]. The following formula is used to convert radiance to ToA reflectance as

$$P_\lambda = \frac{\pi L_\lambda d^2}{ESUN_\lambda \times Cos\theta_z} \quad (3)$$

where P_λ = ToA reflectance [unitless], π = 3.14159, d is the Earth-Sun distance [astronomical units], $ESUN_\lambda$ is the mean exo-atmospheric solar irradiance [W/(m^2 μm)], Θ_z is the Solar zenith angle [degrees].

For images from Landsat OLI, you can directly convert DN into ToA reflectance according to equation 4 (U.S. Geological Survey, 2019).

$$P_\lambda = \frac{M_p \times Q_{cal} + A_p}{Sin\theta_z} \quad (4)$$

where M_p is the reflectance multiplicative scaling factor for the band [unitless], and A_p is the reflectance additive scaling factor for the band [unitless]. The metadata file associated with LANDSAT imagery includes values for parameters such as Q_{cal}, Q_{calmax}, Q_{calmin}, $LMIN_\lambda$, $LMAX_\lambda$, M_p, A_p, and Θ_z (U.S. Geological Survey, 2019).

Digital index

The NDWI index is a useful tool for spotting water bodies on the Earth's surface. The NDWI was determined by using the green and near-infrared bands, as shown in equation 5 (Hossain *et al.* 2021).

The NDWI can range from -1 to +1. The NDWI image typically indicates a good result for areas with water and a bad result for areas without water. To show the boundary between land and water as a coastline, we marked the land features with a 0 and the water features with a 1.

$$NDWI = \frac{(\text{Green}_{\text{BOA}} - \text{NIR}_{\text{BOR}})}{(\text{Green}_{\text{BOA}} + \text{NIR}_{\text{BOA}})} \quad (5)$$

Table II. Major attributes of shoreline and Baseline, uncertainty zero is held as the default value on the DSAS application, and the baseline has been manually created using ArcMap.

OBJECT ID	OBJECT NAME	DATE	UNCERTAINTY	SHAPE LENGTH(m)
1	Shoreline	11/10/1991	0	24387.26
2	Shoreline	11/26/2000	0	22155.80
3	Shoreline	11/22/2010	0	23498.42
4	Shoreline	12/22/2021	0	24309.16
5	Baseline	NA	0	27335.50

DSAS tool for shoreline change analysis

The Digital Shoreline Analysis System (DSAS) Version 6 is the latest standalone software developed for shoreline change analysis. Unlike its earlier versions, which operated as an extension of ArcGIS, DSAS v6 is no longer tied to ArcGIS, offering users more flexibility and independence from GIS software constraints. This modern version integrates a user-friendly interface with enhanced features, making it a powerful and comfortable tool for analyzing coastal changes. It requires pre-processed shoreline data and a baseline in GeoJSON format, ensuring standardized and efficient input handling. With updated algorithms and capabilities, DSAS v6 delivers accurate results, making it ideal for shoreline management and research applications. It estimates common uncertainty 10 and provides 13 types of statistical results that are so effective for analysts.

Varieties of Statistical Methods applied for understanding the Rate of Shoreline Movement

The Shoreline Change Envelope (SCE) and the rate of shoreline change were measured using the EPR, NSM, LRR, and WLR methods as outlined in the Digital Shoreline Analysis System (DSAS). These measurements are commonly used in statistics that track changes along the shoreline.

The End Point Rate (EPR) is the best method when it is calculated using just two shoreline positions at different times (Sarwar and Woodroffe, 2013). The EPR method calculates how much the shoreline changes by dividing the distance by the number of years, as shown in equation six.

$$EPR = \frac{D_1 - D_2}{t_1 - t_0} \quad (6)$$

The distance (m) between the newest and oldest shoreline is represented by $D_1 - D_2$, and the time gap (years) between the two shoreline positions is shown as $t_1 - t_0$.

On the other hand, LRR (Linear regression method) is more appropriate when the number of shorelines exceeds two. OBrien *et al.* (2014) utilized the following LRR formula (Equation 7) for long-term shoreline analysis

$$Y = a + bX \quad (7)$$

In this equation, y represents the distance (in meters) from the baseline. The variable is the starting point of y, while b shows the slope of the line that describes how the shoreline changes over time.

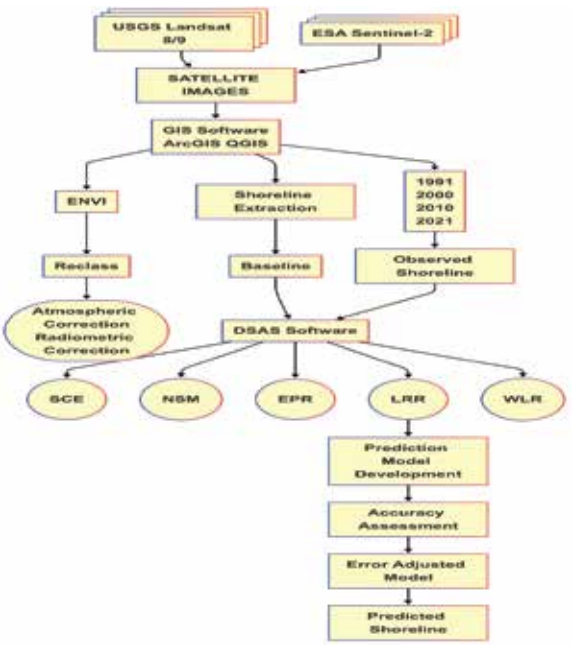

Fig. 3. Schematic flow chart of the overall approach for this research

The variable x stands for the shoreline position in various years. A ±5 m uncertainty and a 95% confidence interval were set as default parameters for statistical calculations. Linear regression involves several key aspects: (1) it uses all available data, no matter if there are changes in trends or accuracy, (2) it relies entirely on calculations, (3) it follows recognized statistical principles, and (4) it is simple to use (*Crowell et al.* 2018). The linear regression method can be affected by outliers and often underestimates how quickly things change compared to other statistics, like EPR (Dolan, 1991).

The Weighted Linear Regression (WLR) method employs a linear regression approach similar to the Linear Regression Rate (LRR) method but incorporates a weighting factor (Equation 8) applied to Equation seven to account for positional uncertainty (Himmelstoss *et al.* 2021).

$$w = \frac{1}{e^2} \tag{8}$$

In the DSAS tool, Hossain *et al.* (2021) utilized the R^2 value to be determined for LRR and WLR methods as presented in Eq.9, and it represents the accuracy and perfection between linear regression rate and weighted linear regression rate.

$$R^2 = 1 - \sqrt{\frac{\sum y - \acute{y}}{\sum y - \bar{y}}} \tag{9}$$

Where y = distance from baseline and known shoreline position, y′= predicted value of the best-fit regression line according to the equation, y = mean of the shoreline position data. The R-squared value, denoted as LR^2, evaluates how well the shoreline position data fits the linear regression line.

Forecasting model

This model (Equation 10) calculates the adjusted shoreline position by incorporating the rate of shoreline movement (LRR) over a given time period. It uses the original intersect point position and adjusts it by multiplying the Linear Regression Rate (LRR), which represents the rate of shoreline change per year, by the time elapsed. This adjustment accounts for both erosion (negative LRR) and accretion (positive LRR), ensuring that the shoreline's movement landward or seaward is accurately represented (Crowell *et al.* 1997). The model can be applied separately to the X and Y coordinates, allowing for a comprehensive adjustment in both directions, and is useful in predicting future shoreline positions or validating trends of coastal change observed over time.

$$X_{new} = X_{origin} + (LRR \times \Delta t) \tag{10}$$

$$Y_{new} = Y_{original} + (LRR \times \Delta t)$$

Where:

X_{new} : Adjusted shoreline position.

$X_{original}$: Original intersect point position.

LRR: Linear Regression Rate (rate of change in shoreline position per year).

Δt represents the time span.

Validation of the Shoreline Prediction Model

The root mean square error is the square root of the variance of the residuals. It shows how well the model fits the data, i.e., how close the actual data points are to what the model predicted Lower RMSE values indicate a better fit, while higher values mean there is more error. The RMSE was used to check how well the actual coastline change rates matched the predicted ones. In shoreline observation, Uddin and Niloy (2022) assessed the calculated model and satellite observations of the shoreline change rate for 2021 by using RMSE values (Equation 11).

Land loss and land gain computation

$$RMSE = \sqrt{\frac{1}{n}\left(\sum_{i=1}^{n}(x_m - x_a)^2 + \frac{1}{n}\sum_{i=1}^{n}(y_m - y_a)^2\right)} \tag{11}$$

The areas identified as water or non-water in the images were compared to find out the values of land loss and gain, using the ArcGIS raster calculator tool (Mullick *et al.* 2019). The changes in land, both lost and gained, were measured over four years in a row, covering a total period of 30 years from 1991 to 2021.

Results and discussion

The general view begins by describing the analysis of 179 transects, with 174 considered active, along an approximately 25 km shoreline. This study utilized Weighted Linear Regression Rate (WLR) and Linear Regression Rate (LRR) for long-term analysis (1991–2021) and End Point Rate (EPR) and Net Shoreline Movement (NSM) for short-term intervals (1991–2000, 2000–2010, and 2010–2021).

Long term observation

Long-term observation includes overall analyses over the past 30 years from 1991 to 2021. There are a number of statistical methods developed to analyze long-term observation (more than two years) involving LRR, WLR, SCE, etc.

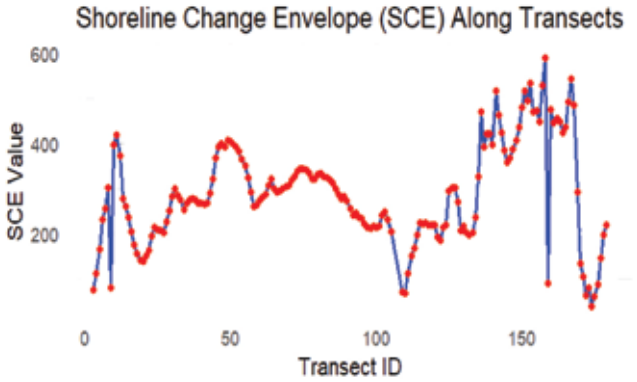

Graph 1. Shown furthest and nearest change over 30 years

Shoreline change envelope

The highest distance range, from 590.78 to 495.79, belongs to the eastern region of shorelines (Graph 1, Fig 4). The farthest distance from the baseline belongs to the range of transect ID from 170 to 150. The nearest distance from the graph lies to the most eastward crossed 170 transect Id (Graph 1, Fig. 4).

Rate of shoreline movement

The Weighted Linear Regression (WLR) method shows varying rates of shoreline change along the studied coastal stretch. The spatial and temporal assessment of shoreline change across zones AB (Western), BC (Central), and CD (Eastern) of the Bay of Bengal reveals distinct patterns of erosion and accretion over the 30-year study period (1991-2021).

Spatial variation in shoreline dynamics

As shown in Fig. 6, the Bay of Bengal coastline demonstrates significant zonal heterogeneity in shoreline change. Zone AB (Western Zone) exhibits a mixed pattern with predominantly erosional transects (73.33%), particularly in its central segment, though some accretional areas (15.56%) appear toward the boundaries. Zone BC (Central Zone) represents the most severely eroded region, with an overwhelming 98.31% of transects classified as erosional and no accretional transects observed. In contrast, Zone CD (Eastern Zone) displays a markedly different pattern with a majority of accretional transects (54.29%) concentrated in its central portion, though erosional processes still affect 28.57% of the area.

Quantitative assessment of shoreline change

The magnitude of shoreline change varies considerably across the study area, as illustrated in Table III. Zone BC exhibits the highest mean erosion rate (-9.48 m/yr), followed by Zone AB (-5.87 m/yr), while Zone CD shows net accre-

Fig. 4. Graphical visualization of the map of shoreline change frequency over 30 years, demonstrating the level of fluctuation. The map has been shown into two major areas, one is the western zone (left) and another one is the eastern zone (right)

tion with a mean shoreline change of +5.88 m/yr. Maximum shoreline retreat was recorded in Zone BC (-13.8 m/yr), closely followed by Zone AB (-13.12 m/yr). Conversely, Zone CD registered the most substantial accretion, with a maximum shoreline advance of +25.58 m/yr, highlighting the dynamic nature of this eastern segment.

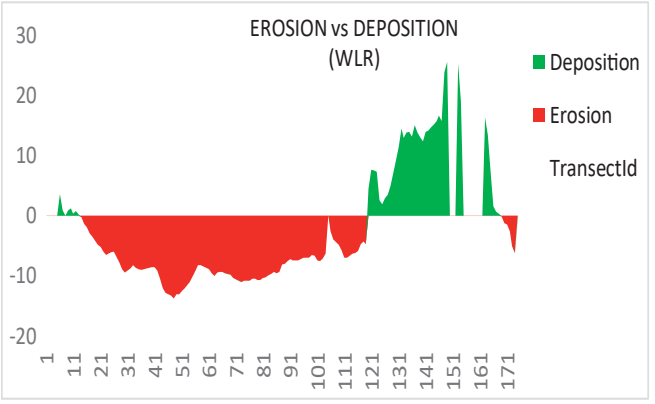

Graph 2. Erosion and deposition rate per year along transect

Transect-wise analysis

Graph 2 provides a detailed transect-by-transect visualization of erosion versus deposition patterns. The predominance of erosional processes (red areas) is evident across transects 1-120, corresponding primarily to Zones AB and BC. The pronounced erosional trough between transects 43-64 corresponds to the area of maximum retreat in Zone AB.

A dramatic shift occurs around transect 127, where substantial depositional processes (green areas) begin to dominate, reaching peak values exceeding +20 m/yr at transects 148-152, which aligns with the central portion of Zone CD. Notable interruptions in the accretional pattern occur around transects 155-158 and 168-169, indicating localized erosional hotspots within the generally accretional eastern zone.

Short term observation

Shoreline variation is observed for each 10-year period from 1991 to 2021. The Fig. 6 shows seaward and landward movement at Kuakata area, Bay of Bengal, across three periods: 1991–2000, 2000–2010, and 2010–2021. Accretion dominates in the eastern region, while erosion is prevalent in the western section, particularly post-2000. In terms of short-period observation, the number of green transects is increasing both eastward and It reaches a peak point in 2021 from both the east and west portions, as shown in graph. 3 and Fig. 6. The method for frequent analyses is followed by NSM (Net Shoreline Movement) and EPR (End Point Rate).

Table III. Quantitative assessment of shoreline movement across three zones

Descriptive statistics	Zone AB	Zone BC	Zone CD	Total
Total transects	45	59	70	174
Total Erosional Transects	33	58	20	111
Total Accretional transects	07	00	38	45
Total Stable transects	00	01	12	00
Undefined transects	05	00	00	18
Erosional transects (%)	73.33	98.30	28.57	63.79
Accretional transects (%)	15.56	00	54.28	25.86
Mean shoreline change	-5.87	-9.47	5.87	-2.84
Max shoreline change	3.6	-6.35	25.58	25.58
Min shoreline change	-13.12	-13.80	-7.02	-13.80
Mean erosion	-5.40	-9.31	-1.30	-5.07
SD erosion	4.21	2.21	2.32	4.49
Mean accretion	0.18	00	6.17	2.54
SD accretion	0.60	00	7.47	0.31

Table IV. Showing quantitative values of seaward (positive value) and landward (negative value) movement, over every ten-year period with an overall 30-year period

Descriptive Statistics	Period (1991 to 2000)	Period (2000 to 2010)	Period (2010 to 2021)	Period (1991 to 2021)
Total number of Transects	140	136	162	174
Average Rate	-9.68	-0.98	2.10	-2.84
Number of Erosional Transects	123	101	99	111
Erosional Transects (%)	87.86	74.26	61.11	63.80
Average Erosional Rates	-13.11	-6.42	-8.38	-5.08
Maximum Value Erosion	-24.50	-15.49	-14.64	-13.80
Number of Accretional Transects	17	35	63	45
Accretional Transects (%)	12.14	25.74	38.89	25.86
Average Accretional Rates	15.09	14.73	18.56	2.54
Maximum Value Accretion	33.49	40.34	44.90	25.58

Quantitative analysis using the EPR (End Point Rate) method

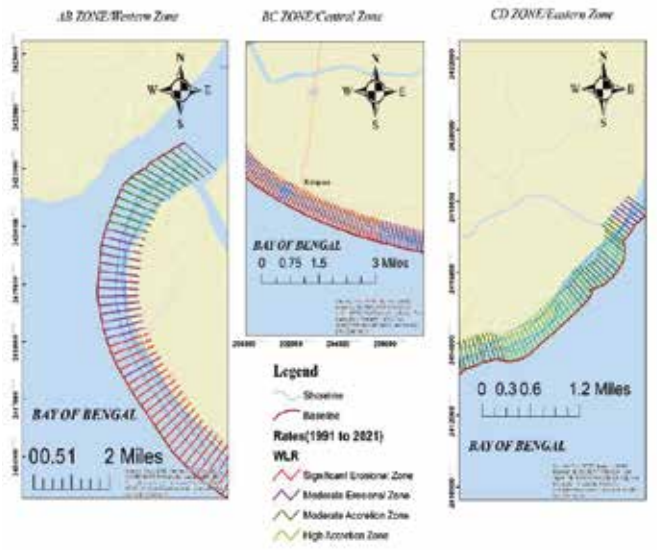

Fig. 5. Map of three zones showing their transect rate

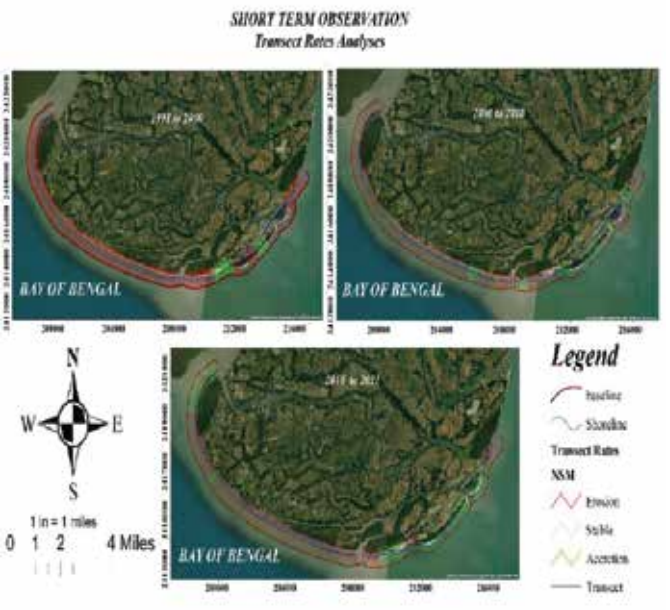

Fig. 6. Three periodical maps for understanding seaward and landward movement patterns

The End Point Rate (EPR) analysis is presented across three time periods: 1991-2000, 2000-2010, and 2010-2021. The Graph 3 and the Table IV demonstrate predominantly erosional rates with peaks reaching more than -20 meters/-year, though a notable accretion peak of about more than 30 meters/year appears around transect 125 between 1991 and 2000.

The 2000-2010 period exhibits similar erosional trends in the central part of the transects but displays a significant accretion peak of nearly 40 meters/year around transect 125 (Table IV). The most recent period (2010-2021) shows a more variable pattern with two distinct accretion peaks: one at the beginning of the stretch (around transect 15) reaching approximately 35 meters/year (Graph 3), and another more

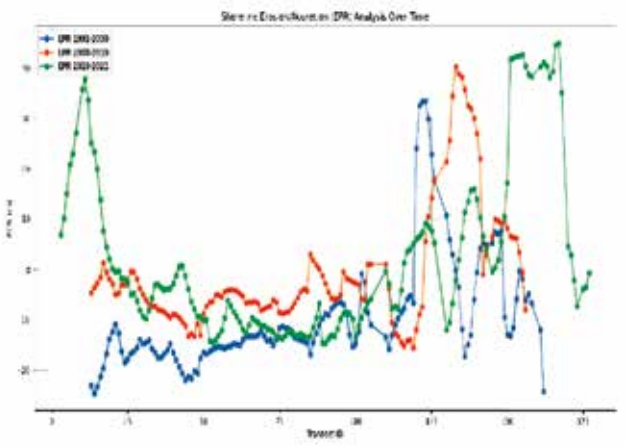

Graph 3. Per year positional variation of three shorelines along transects

pronounced peak near transect 175 reaching about 44.9 meters/year, as shown in Table IV, and Graph 3. All three time periods demonstrate fluctuating patterns of shoreline change rates across the study area, with the magnitude and location of peaks varying between periods. The average rate of shoreline change shows a progressive shift from erosional dominance to accretional tendency, changing from -9.68 m/year (1991-2000) to -0.98 m/year (2000-2010), and finally to 2.1 m/year (2010-2021), in Table IV, which supports Fig. 8.

average depositional rates increased from 15.09 m/year to 18.56 m/year across the study period.

Computation of land loss and land gain

In Fig. 7, the analysis of shoreline movement (NSM) along the Bay of Bengal coast revealed distinct patterns of morphological changes across three temporal periods: 1991-2000,

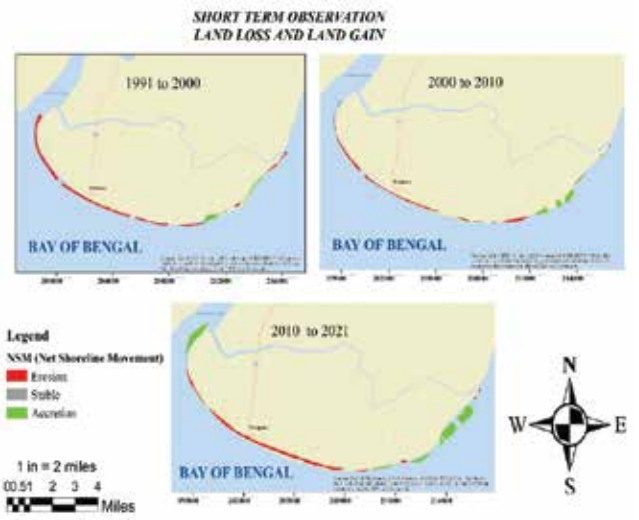

Fig. 7. Three maps of shorelines over three times showing their sediment loss and gain

Table V. Quantitative values of sedimentation and sediment removal

Descriptive Statistics	Period (1991 to 2000)	Period (2000 to 2010)	Period (2010 to 2021)	Total
Sum of Area (Km^2)	4.60	2.85	5.81	13.27
Average of Area(Km^2)	0.03	0.02	0.03	0.09
Erosional Area(Km^2)	3.87	1.71	2.54	8.13
Mean Erosional Area(Km^2)	0.03	0.01	0.02	0.07
Accretional Area(Km^2)	0.72	1.14	3.27	5.14
Mean Accretional Area(Km^2)	0.04	0.03	0.051	0.13
Non-transectional Area(Km^2)	0.0007	0.0001	0.00003	0.0009

The number of erosional transects decreased over time from 123 (87.86%) in 1991-2000 to 99 (61.11%) in 2010-2021, while depositional transects increased from 17 (12.14%) to 63 (38.89%) during the same period. Maximum erosion rates decreased from -24.5 m/year to -14.64 m/year, while maximum accretion rates increased from 33.49 m/year to 44.9 m/year. The average erosional rates moderated from -13.11 m/year to -8.38 m/year, while

2000-2010, and 2010-2021. The shoreline exhibited both erosional and accretional trends, with varying intensities along different coastal segments. During 1991-2000, the coastline was predominantly characterized by erosion (indicated in red), particularly along the central portion of the study area.

A small section in the eastern segment showed accretion (shown in green), while isolated stable areas (indicated in grey) were observed intermittently along the shoreline. The period 2000-2010 demonstrated a similar erosional pattern, though with some notable changes. The extent of erosion remained significant along the western and central sections, while the eastern portion showed increased accretional tendencies compared to the previous decade. The stable zones appeared to be more fragmentary during this period.

The most recent period (2010-2021) exhibited a continuation of the erosional trend along the western and central coastline. However, the eastern section displayed enhanced accretion, suggesting a persistent pattern of sediment accumulation in this area. The transition between erosional and accretional zones appeared more distinct compared to earlier periods. The analysis of shoreline movement (NSM) along the Bay of Bengal coast revealed significant morphological changes across three temporal periods: 1991-2000, 2000 2010, and 2010-2021. The total affected area over the entire study period was 13.27 km², indicating substantial coastal dynamics in the region, as mentioned in Table V and Graph 4.

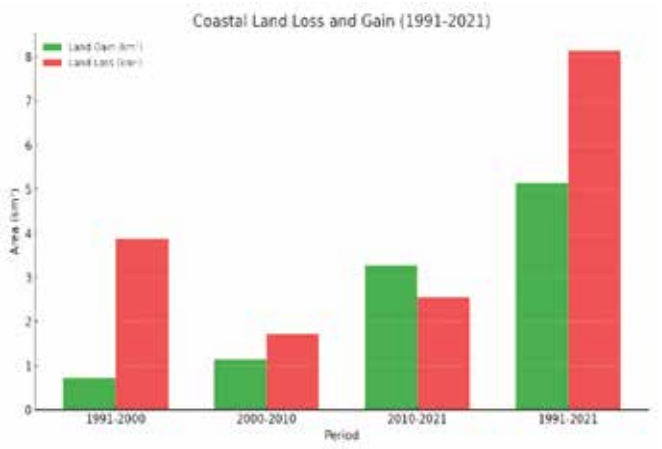

Graph 4. Bar chart of sediment gain and sediment loss

Expected shoreline position

According to Fig. 8, these historical trends manifest in distinct spatial patterns. The eastern portion, however, exhibits a significant landward movement, indicating persistent erosional processes despite the overall increase in previous erosional transects.

This spatial variation in shoreline movement suggests that while accretional processes at the central zone have increased over time at a broader scale, localized erosional hotspots persist, particularly in the eastern section.

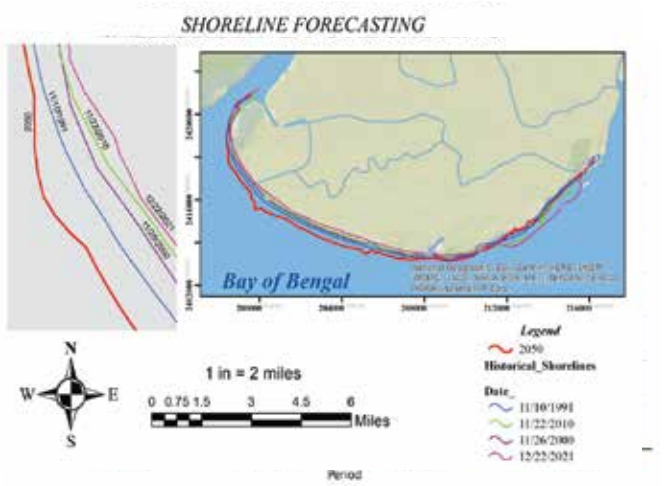

Fig. 8. Expected Shoreline Position after 29 years from 2021

A remarkable morphological change along the coastline was observed with high fluctuation in some coastal zones from 1991 to 2021. These physiological changes along the Bay of Bengal at Kuakata experienced both erosion and deposition, along with inward and outward movement of the shoreline. This study has highlighted both long-term observation over one period from 1991 to 2021 and short-term observation into three periods with a 10-year interval.

A comparable study conducted by Goswami *et al.* (2022) analyzed 1052 transects over a 55 km shoreline of Kuakata area, employing metrics such as EPR, NSM, and LRR while integrating SCE to assess shoreline variability over 20 years from 2000 to 2020. Another study by Islam *et al.* (2014) found, in their study on Kutubdia Island, south eastern zone of Bangladesh, a strong correlation between EPR with WLR and LRR. However, their prime result of the transect rates is 0.29 m/yr, 2.91m/yr, and 3.53 for EPR, LRR, and WLR, respectively.

Similar studies conducted in the same location by Bushra *et al.* (2021), their studies strongly supported our findings, though they chose a bit longer distance toward the north part from the Golachipa River at the eastern side. They got lost area of approximately 13.59 km², over 30 years from 1989 to 2020, likely, in my studies (Table V, Graph. 4) loss of area is more than 8 km².

On the side of Red Crab Island in south eastern zone, it is literally being sedimentation from past years according to all previous publications and our research as well (Fig. 7). In this study, the shoreline dynamics along the Kuakata

coast from 1991 to 2021 revealed significant erosion patterns, consistent with the findings of Uddin & Niloy (2022). Their investigation results have clarified that red crab char, the eastern part of Kuakata beach, is more dynamic, demonstrating a vulnerable region and high SCE is 486m from Uddin and Niloy (2022) and 490 in order to this report (Graph. 1, Fig. 4). My study found higher overall shoreline loss (~8.2 km²) and gain (~5.3 km²) compared to their 6.11 km² loss and 3.26 km² gain. Differences may arise from data sources and methodology, but both studies indicate a long-term erosional trend. On the side of statistical rate of shoreline variation, max, and min shoreline change rates regarding three zones (Table III) are homogenized by them, for instance, mean coastline variation -2.84 from our study and -3.11 in order to Uddin and Niloy (2022), similarly, highest accretion rate from CD altered section shows insignificant difference as from my study is 25.58 and 23.88 from their study. Overall, it can be observed that no significant variation is found between the studies.

Coastal districts are evaluated considering temporal shoreline change analyses by Shamsuzzoha and Tofael (2023), and they analyzed the whole southern part of Bangladesh altogether, with a different approach, which poses challenges to making comparisons.

Shoreline forecasting has been limited, primarily for identifying critical areas. Rahman and Ferdous (2019) and Uddin & Niloy (2022) predicted shorelines for 2028 and 2041, while this study forecasts 2050 (Fig. 8). Rahman and Ferdous (2019) analyzed the entire northern Bay of Bengal, making a Kalapara-specific evaluation difficult. Uddin and Niloy (2022) used DSAS beta forecasting, differing from this study's equation-based model (equation_10), which aligns with observed short-term trends (1991–2021). The central part of Kuakata is predicted to shift seaward, which is in contrast findings of Uddin and Niloy (2022), while the eastern part will experience significant landward movement, partially aligning with previous findings. However, uncertainties remain due to the long projection period (29 years) and using a different prediction model, making the forecast probabilistic rather than absolute.

Notably, the southeastern zone, which includes Red Crab Island (or char), appears to be highly dynamic, with significant landward shoreline movement indicating erosion. This region's vulnerability may stem from its exposure to high-energy tidal forces and sediment-starved conditions, leading to the gradual loss of land (Uddin and Niloy, 2022). The ecological significance of Red Crab Island, coupled with its role as a potential buffer against coastal erosion, makes it a critical area for focused conservation and monitoring efforts.

Conclusion

This study provides a comprehensive analysis of shoreline dynamics along the Kuakata coast, Bangladesh, over a 30-year period (1991–2021). Using multi-temporal Landsat imagery and the Digital Shoreline Analysis System (DSAS), key findings revealed the highest erosion rate of -13.8 m/year in the central BC part and the highest accretion rate of +25.58 m/year in the southeastern zone.

These findings underscore the dynamic nature of the Kuakata coastline, and due to our ignoring a direct field visit, we could not detect the exact reason among many probable reasons, including climate change, anthropogenic activities, tidal flux, etc. The study highlights the vulnerability of coastal communities and infrastructure, necessitating immediate action to mitigate erosion risks and promote sustainable development.

Future research should focus on discontinuous areas, deep social impact with accurate reasons, and detecting the exact reason by integrating higher-resolution satellite imagery, field validation, and hydrodynamic modeling.

Acknowledgement

Special thanks to the supervisor, Professor Mohammad Zahedur Rahman Chowdhury, for his close cooperation and guidance throughout, and parents for their mental and financial support.

References

Alam R, Saiful IM, Raqubul HM and Zahirul HKM (2014), Characteristics of hydrodynamic processes in the Meghna Estuary due to dynamic whirl action. *IOSR Journal of Engineering* **4**: 3-39. Retrieved from http://www.iosrjen.org.

Anwar S, Rahman K and Bhuiyan AE (2022), Assessment of sea level and morphological changes along the eastern coast of Bangladesh, *Journal of Marine Science and Engineering* **10**: 527. https:// doi.org/ 10.3390/ jmse 10040527.

Astiti SPC, Osawa T and Nuarsa IW (2019), Identification of shoreline changes using Sentinel 2 imagery data in Canggu coastal area. ECOTROPHIC: Jurnal Ilmu Lingkungan, *Journal of Environmental Science*, **13**(2): 191-198. https://doi.org/10.24843/ EJES.2019. V13.I02.P07.

Brammer H (2014), Bangladesh's dynamic coastal regions and sea-level rise, *Climate Risk Management* **1:** 51-62. https://doi.org/ 10.1016/J.CRM.2013.10.001

BBC (Bangladesh Bureau of Statistics) (2022), Population and Housing Census 2022: Preliminary Report. Statistics and Informatics Division, Ministry of Planning, Government of the People's Republic of Bangladesh. Retrieved from https://bbs.gov.bd/site/page/47856ad0-7e1c-4aab-bd78-892733bc06eb/Population-and-Housing-Census.

BBC (Bangladesh Bureau of Statistics) (2011), Population and Housing Census 2011: Preliminary Report. Statistics and Informatics Division, Ministry of Planning, Government of the People's Republic of Bangladesh. Retrieved from https://bbs.gov.bd/site/page/47856ad0-7e1c-4aab-bd78-892733bc06eb/Population-and-Housing-Census.

Bushra N, Mostafiz RB, Rohli RV and Friedland CJ (2021), Technical and social approaches to study shoreline change of Kuakata, Bangladesh, *Frontiers in Marine Science* **8**: 1-13. https:// doi.org/ 10.3389/ fmars. 2021.730984

BMD (Bangladesh Meteorological Department) (2020), Annual climate summary, Dhaka: Bangladesh Meteorological Department. Retrieved from https://www.bmd.gov.bd/

Basheer AKK and Pandey AC (2022), Assessment and prediction of shoreline change using multi-temporal satellite data and geostatistics: A case study on the eastern coast of India, *Journal of Water and Climate Change* **13**(3): 1477-1493. https://doi.org/10.2166/wcc.2022.270

Bangladesh Tide Times, High and Low Tide Table, Fishing Times (2024), Retrieved December 22, from https://www.tideschart.com/Bangladesh/#google_vignette

Crowell M, Douglas BC and Leatherman SP (1997), On forecasting future U.S. shoreline positions: A test of algorithms, *Journal of Coastal Research* **13**(4): 1245-1255. https://www.jstor.org/stable/4298734

Chander G, Markham BL and Helder DL (2009), Summary of current radiometric calibration coefficients for Landsat MSS, TM, ETM+, and EO-1 ALI sensors, *Remote Sensing of Environment* **113**(5): 893-903. https://doi.org/10.1016/J.RSE.2009.01.007

Crowell M, Leatherman SP and Douglas B (2018), Erosion: Historical analysis and forecasting. *Encyclopedia of Coastal Science*, pp 792-798. https://-doi.org/10.1007/978-3-319-93806-6_138

Dolan R, Fenster MS and Holme SJ (1991), Temporal analysis of shoreline recession and accretion, *Journal of Coastal Research* **7**(3): 723-744.

Fejjari A, Valentino G, Briffa JA and D'Amico S (2023), Detection and monitoring of maltese shoreline changes using sentinel-2 Imagery. *2023 IEEE International Workshop on Metrology for the Sea; Learning to Measure Sea Health Parameters, MetroSea - Proceedings*, pp 52-56. https://doi.org/10.1109/METROSEA58055. 2023.10317486

Goswami S, Rahman SA, Alam MT, Rahman M, Rafiq R, Jaman H and Roy DK (2022), Assessment of shoreline changes and the groundwater quality along the coast of Kuakata, Patuakhali, Bangladesh. *Journal of Ecological Engineering* **23**(7): 323–332. http://doi.org/ 10.12911/ 22998993/149938.

Hossain S, Yasir M, Wang P, Ullah S, Jahan M, Hui S and Zhao Z (2021), Automatic shoreline extraction and change detection : A study on the southeast coast of Bangladesh, *Marine Geology* **441**: 106628. https://-doi.org/10.1016/j.margeo.2021.106628

Hoque E, Chowdhury SR and Zahedur M (2021), Morphological changes of a developing sandbar along the shoreline of Sonadia Island, Bangladesh between 1972 and 2006 using remote sensing. *Geology, Ecology, and Landscapes* 7(1): 87-95. https://doi.org/ 10.1080/ 24749508. 2021.1923290

Himmelstoss EA, Henderson RE, Kratzmann MG and Farris AS (2021), Digital Shoreline Analysis System (DSAS) Version 5.1 User Guide: U.S. Geological Survey Open-File Report 2021–1091. *U.S. Geological Survey*. Retrieved from https://doi.org/10.3133/ofr20211091

Islam K, Hasan M, Rahman M, Fayyaz R and Hamid T (2022), Shoreline dynamics assessment of Moheshkhali Island of Bangladesh using Integrated GIS-DSAS techniques, *The Dhaka University Journal of Earth*

and Environmental Sciences **11**(1): 1–14. https://-doi.org/10.3329/dujees. v11i1.63707

Islam MA, Hossain MS, Hasan T and Murshed S (2014), Shoreline changes along the Kutubdia Island, south-east Bangladesh using digital shoreline analysis system, *Bangladesh Journal of Scientific Research* **27**(1): 99-108. https:// doi.org/ 10.3329/ bjsr.v27i1.26228

Kabir A and Tanvir K (2020), Assessing the shoreline dynamics of Hatiya Island of Meghna estuary in Bangladesh using multiband satellite imageries and hydro-meteorological data. *Regional Studies in Marine Science* **35**: 101167. https://doi.org/10.1016/j.rsma.2020.101167

Macro Trends (2024), Bangladesh Population 1950-2025. Retrieved 2024, from https://www.macrotrends.net/-global-metrics/countries/BGD/bangladesh/population

Mullick RA, Islam KMA and Tanim AH (2019), Shoreline change assessment using geospatial tools: a study on the Ganges deltaic coast of Bangladesh. Earth Science Informatics **12**(3): 299–217. https://doi.org/10.1007/ s12145- 019-00423-x

Maiti S and Bhattacharya AK (2009), Shoreline change analysis and its application to prediction: A remote sensing and statistics based approach. *Marine Geology* **257**(1-4): 11–23. https://doi.org/10.1016/J.MAR-GEO.2008.10.006

O'Brien K, Stocker J, Hyde B and Barrett J (2014), Analysis of shoreline change in Connecticut: 100 Years of erosion and accretion. *Connecticut Sea Grant & UCONN Center for Land Use Education and Research (CLEAR), Connecticut Department of Energy & Environmental Protection*, Retrieved from NOAA Repository

Paul BK and Rashid H (2016), Climatic Hazards in Coastal Bangladesh: Non-Structural and Structural Solutions. Elsevier Inc. Retrieved from https://www.sciencedi-rect.com/book/9780128052761/climatic-haz-ards-in-coastal-bangladesh

Rahman MTU and Ferdous J (2019), Geomorphological changes along coastline of Bangladesh. *2nd International Conference on Water and Environmental Engineering (iCWEE2019)*, Dhaka.

Rose L and Bhaskaran PK (2017), Tidal asymmetry and characteristics of tides at the head of the Bay of Bengal. *Quarterly Journal of the Royal Meteorological Society* **143**(708): 2735-2740. https://doi.org/10. 1002/QJ.3122

Sarwar GM and Woodroffe CD (2013), Rates of shoreline change along the coast of Bangladesh, *Journal of Coastal Conservation* **17**(3): 515-526. https://-doi.org/10.1007/ s11852-013-0251-6

Shamsuzzoha M and Ahamed T (2023), Shoreline change assessment in the coastal region of Bangladesh delta using tasseled cap transformation from satellite remote sensing dataset, *Remote Sensing* **15**: 295. https://-doi.org/10.3390/rs15020295

UHSLC (University of Hawaii Sea Level Center) (2024), UHSLC Stations. Retrieved from https:// uhslc.soest. hawaii.edu/stations/?stn=124#levels

U.S. Geological Survey (2019), Landsat 8 Data Users Handbook. U.S. Geological Survey. Retrieved from https://landsat.usgs.gov/documents/Landsat8DataUs-ersHandbook.pdf

Uddin J and Niloy NR (2022), Assessing the shoreline dynamics on Kuakata, coastal area of Bangladesh: a GIS- and RS-based approach, *Arab Gulf Journal of Scientific Research* **41**(3): 240-259. https://-doi.org/10.1108/AGJSR-07-2022-0114

Uddin K, Khanal N, Chaudhary S, Maharjan S and Thapa RB (2020), Coastal morphological changes: Assessing long-term ecological transformations across the northern Bay of Bengal, *Environmental Challenges* **1**: 100001. https://doi.org/10.1016/j.envc.2020.100001